Available online at www.sciencedirect.com
SCIENCE DIRECT®
Atmospheric Environment 39 (2005) 1049–1068
ATMOSPHERIC ENVIRONMENT
www.elsevier.com/locate/atmosenv

A comparison of contaminant plume statistics from a Gaussian puff and urban CFD model for two large cities

Julie Pullen[a,*], Jay P. Boris[b], Theodore Young[b], Gopal Patnaik[b], John Iselin[c]

[a]*Center for International Security and Cooperation, Stanford University, Stanford, CA 94305, USA*
[b]*Laboratory for Computational Physics and Fluid Dynamics, Naval Research Laboratory, Washington DC 20375, USA*
[c]*Bucknell University, Lewisburg, PA 17837, USA*

Received 29 February 2004; received in revised form 6 October 2004; accepted 6 October 2004

Abstract

This paper quantitatively assesses the spatial extent of modeled contaminated regions resulting from hypothetical airborne agent releases in major urban areas. We compare statistics from a release at several different sites in Washington DC and Chicago using a Gaussian puff model (SCIPUFF, version 1.3, with urban parameter settings) and a building-resolving computational fluid dynamics (CFD) model (FAST3D-CT). For a neutrally buoyant gas source term with urban meteorology, we compare near-surface dosage values within several kilometers of the release during the first half hour, before the gas is dispersed beyond the critical lethal level. In particular, using "fine-grain" point-wise statistics such as fractional bias, spatial correlations and the percentage of points lying within a factor of two, we find that dosage distributions from the Gaussian puff and CFD model share few features in common. Yet the "coarse-grain" statistic that compares areas contained within a given contour level reveals that the differences between the models are less pronounced. Most significant among these distinctions is the rapid lofting, leading to enhanced vertical mixing, and projection downwind of the contaminant by the interaction of the winds with the urban landscape in the CFD model. This model-to-model discrepancy is partially ameliorated by supplying the puff model with more detailed information about the urban boundary layer that evolves on the CFD grid. While improving the correspondence of the models when using the "coarse-grain" statistic, the additional information does not lead to quite as substantial an overall agreement between the models when the "fine-grain" statistics are compared. The taller, denser and more variable building landscape of Chicago created increased sensitivity to release site and led to greater divergence in FAST3D-CT and SCIPUFF results relative to the flatter, sparser and more uniform urban morphology of Washington DC.

Keywords: Urban dispersion; Urban meteorology; Emergency response; Modeling

1. Introduction

Hosker (1984, 1987) recognized that the mechanical forcing of flow around buildings spawns distinctive features like lee eddies, vortex shedding and "urban canyons". Recent urban field and modeling campaigns in medium size cities (Urban 2000 and Urban 2003) have

*Corresponding author. Marine Meteorology Division, Naval Research Laboratory, 7 Grace Hopper Dr. Stop 2, Monterey, CA 93943, USA. Tel.: +1 831 656 4645; fax: +1 831 656 4769.
E-mail address: pullen@nrlmry.navy.mil (J. Pullen).

1352-2310/$ - see front matter © 2004 Elsevier Ltd. All rights reserved.
doi:10.1016/j.atmosenv.2004.10.043

drawn widespread attention to the intricate small-scale circulation patterns that can develop as winds interact with the urban landscape created by buildings and streets (Allwine et al., 2002). However, there is an additional thermodynamic component to urban flows. These flows are deterministic at the scale of the buildings and are intrinsically convective, not diffusive. Underlying the gross heat island effect (Oke, 1984) are small-scale contributions like the formation of vortices in street canyons due to the differential surface heating of the sidewalls (Oke et al., 1991) which also impacts contaminant transport (Kim and Baik, 1999).

The nascent focus on the real-time use of atmospheric transport and dispersion models for national security raises expectations for accurate models applied to big complex metropolitan settings (NRC, 2003). As the demand for high-fidelity models of large urban environments accelerates, computational advances have not kept pace.

For predicting distribution patterns within a city, a building-resolving CFD model is expected to be unparalleled because it explicitly resolves the relevant physics at the scales of motion and thereby requires minimal parametrizations. Applications that would benefit from such a model include emergency medical response in the immediate aftermath of a release and base or specific building protection. Such a capability would allow rescuers to search the most contaminated portions of a city first and enter buildings as soon as possible after contaminant levels have dropped.

Building-resolving CFD models that explicitly represent the physics on the necessary small scales give detailed results but require significant computing resources and extensive simulation times. Consequently, the operational communities rely on rapidly relocatable relatively simple puff models that ingest limited information about the local meteorology and produce contaminant forecasts (OFCM, 1999). These models tend to generate quite symmetric oval-shaped contaminant footprints, and unfortunately are often insensitive to details of the local urban morphology.

With the microscale meteorological and urban communities intently focused on model validation in medium size non-coastal urban areas (Salt Lake City in Urban 2000 and Oklahoma City in Urban 2003), few high-resolution modeling (CFD) efforts have been mounted for major metropolitan areas. Yet much of the US population lives in big cities along the coasts. Hence there is a pressing need to know to what extent we can rely on operational environmental forecast models when making critical decisions in an emergency when large populations are at risk.

The case studies examined here are designed to probe the differences between a CFD and a puff model by employing several statistical measures to ascertain how these models perform when applied to hypothetical releases in two major urban areas, Washington DC and Chicago. The focus is on timescales on the order of 15 min—which is typically the time within which an emergency response to an airborne chemical release can be most effective (Boris et al., 2002). Chicago buildings are taller on average, more variable in height, and more tightly spaced than the buildings in Washington DC. The impact of this contrast in urban morphology on contaminant distribution will be explored here.

In Section 2, we detail the model configuration and source release specifications. We carry out a model-to-model comparison in the subsequent sections. In Sections 3 and 4, fine- and coarse-grain statistical measures are utilized to compare the puff and CFD model dosage patterns. Section 5 contains a discussion of the agent concentration within the boundary layer. The paper concludes in Section 6.

2. Model configuration

We employ an urban CFD model (FAST3D-CT) developed at the Laboratory for Computational Physics and Fluid Dynamics at the Naval Research Laboratory in Washington DC (Patnaik et al., 2003; Boris, 2002). Originally designed for a range of small-scale fluid dynamic flows including complex flow around ships at sea to assist aircraft landings, the model was successfully evaluated against wind tunnel turbulence experiments (Fureby and Grinstein, 2002). The model solves the high Reynolds number Navier–Stokes equations using a time-dependent, three-dimensional monotone integrated large eddy simulation (MILES) formulation (Oran and Boris, 2001; Boris et al., 1992). This approach has been found to be computationally efficient and adds no extra dissipation (Grinstein and Fureby, 2002). In addition, the model incorporates stochastic backscatter and a fourth-order phase accurate flux-corrected transport finite volume algorithm for detailed building and city aerodynamics. The convective nature of turbulent urban flows is represented in the model physics. Solar heating of surfaces is based on "land use" data tables. Buildings and trees cast shadows (depending on the time of day), and building sides and tops heat the environment (even at night) and transfer heat to the air passing by. Buoyancy is included through a consistent potential temperature computation.

FAST3D-CT, being an LES formulation, responds to time-dependent boundary conditions whose spatial and temporal scales attempt to mimic realistic variability. Coupled with low numerical dissipation, the multi-spectral chaotic fluctuations ensure that turbulent kinetic energy levels are maintained downwind.

FAST3D-CT has been shown to give accurate vortex shedding statistics in a validation study of flow around the Washington monument (Boris, 2002) and in detailed

building studies supported by Lawrence Livermore National Laboratory experiments (Emery et al., 2000). Evaluation of model simulations in an urban environment was conducted using Los Angeles tracer release data. The experimental data was found to be statistically indistinguishable from the distribution of simulated realizations (Boris et al., 2004).

Unfortunately, no field data were available for Washington DC or Chicago. However, efforts to extend the urban evaluation to Oklahoma City and New York City are ongoing. The field data comparison to date contributes to confidence that FAST3D-CT reasonably captures important mechanical and thermal effects of the urban landscape.

For the Washington DC and Chicago simulations presented here, FAST3D-CT used horizontal and vertical resolutions of 6 m. The computational timestep was 0.36 s. The model grid consists of a 1-m resolution

Fig. 1. The downtown portions of the Washington DC (top) and Chicago (bottom) grids. Release sites are marked with a circled cross. Site r1 is the left one in Washington DC, while r1 is the top site in Chicago. Wind direction is shown with a grey arrow. Buildings are contoured at a 5 m height interval.

building database (Patnaik et al., 2003) on a flat terrain. The grid dimensions are $860 \times 580 \times 40$ levels for Washington DC and $360 \times 360 \times 55$ levels for Chicago. For the 3 km^2 interior downtown region (Fig. 1) the mean (standard deviation) of building height is 24.32 m (11.74 m) on the Washington DC grid and 69.54 m (56.43 m) on the Chicago grid. In the region shown in Fig. 1 where most of the contaminant in the model simulations was confined, the buildings cover 25.03% of the area in Washington DC while the buildings comprise 35.28% of the area in Chicago.

Four hypothetical release sites were simulated for each city—one release site at a time. The sites were located in a line along a major urban street with maximum separation of release site 1 (r1) and release site 4 (r4) of 0.52 km in Washington DC and 0.53 km in Chicago. In the Washington DC run, the wind was from -62° (negative is counterclockwise from north, or 0°). In the Chicago simulation the wind came from 83° and was more perpendicular to the line of release sites.

The model initialization was based on available urban observations and represents an analytic realization of a fluctuating (gusting) urban boundary layer. The models were run for at least 5 min before the first agent release occurred. Each hypothetical source consisted of a neutrally buoyant gas having a mass of 10^3 kg (1 ton) and extending 20 m in each dimension. The release was assumed to be centered 10 m above the ground. The release time was taken to be during the afternoon (approximately 3 pm local time) in winter, and each release was instantaneous.

The transport and dispersion component of the Department of Defense's Defense Threat Reduction Agency's (DTRA) Hazard Prediction and Assessment Capability (HPAC) system is the Gaussian puff model, SCIPUFF. SCIPUFF has a second-order turbulence closure and uses a Lagrangian transport algorithm (Sykes et al., 1997). Input data configurations for SCIPUFF were designed to mimic the release scenario described above using the HPAC 3.2.1 interface, with urban settings similar to those that are fixed in "urban HPAC." All simulations used a uniform surface roughness intended to approximate the height of roughness elements encountered in a city ($z_0 = 0.5$, recommended by Sykes et al., 1997).

We have employed SCIPUFF as a representative Gaussian puff model. It has become an "industry standard" due to its foundational role within HPAC and extensive validation work surrounding it (Nappo et al., 1998). An intercomparison of the standard Department of Defense and Department of Energy models (HPAC and NARAC, respectively) showed that for very simple (open field) release scenarios they produced essentially identical contaminant distributions in the plumes (Warner et al., 2001). The documented similarity of operational plume model response to simple source and meteorological specifications serves as a point of departure for interpreting the results presented here.

The sequence of SCIPUFF simulations were selected to supply successively more urban boundary layer information to the puff model. The source of the meteorological information was the area-averaged velocity and velocity fluctuations that evolved on the CFD model grid (Figs. 2,3 and Table 1). In the run labeled "noBL10m" only winds (u and v) at the standard meteorological station height of 10 m were supplied to SCIPUFF from the CFD model. For "noBL35m" only a value of velocity at 35 m, further up in the boundary layer, was specified. In "BLCFD" the full wind velocity profile as a function of height from the CFD model was given to SCIPUFF. Also, an estimate of the urban boundary layer height from the CFD model was prescribed. Finally, in "BLCFDv" the area-averaged,

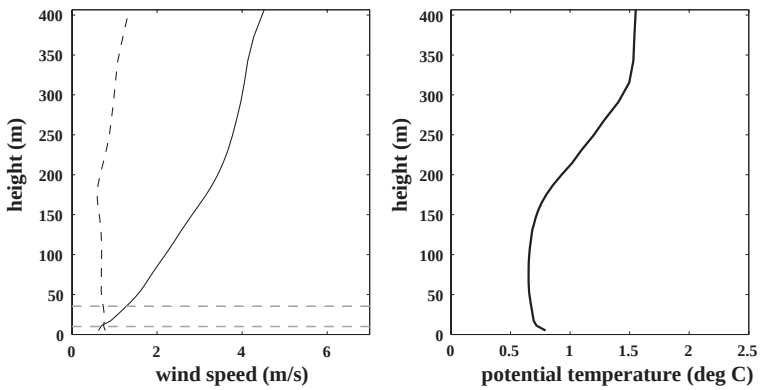

Fig. 2. (Left panel) magnitude of the mean (solid line) and magnitude of the RMS (dashed line) of the area-averaged wind velocity for the FAST3D-CT Washington DC simulation. The observation heights for the SCIPUFF noBL10m and noBL35m simulations are shown by the dashed grey line. (Right panel) area-averaged potential temperature on the CFD grid. The profiles were computed before the end of the 30 min simulation, and after the profiles stopped evolving.

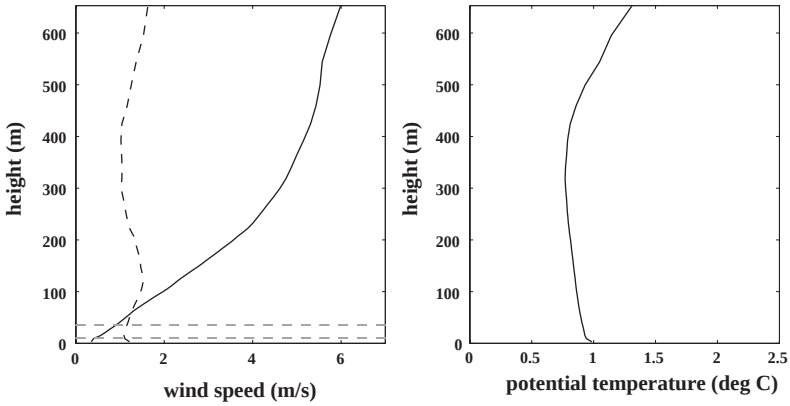

Fig. 3. As in Fig. 2 but for the FAST3D-CT Chicago simulation.

Table 1
Specification of meteorological information from FAST3D-CT to SCIPUFF

	Washington DC	Chicago
noBL10m	10-m velocity: $u = 0.6$, $v = -0.3$	10-m velocity: $u = -0.4$, $v = -0.1$
noBL35m	35-m velocity: $u = 1.1$, $v = -0.6$	35-m velocity: $u = -0.9$, $v = -0.1$
BLCFD	Velocity profile and $z_i = 175$ m	Velocity profile and $z_i = 500$ m
BLCFDv	Velocity profile, $z_i = 175$ m and velocity variance $= 0.75\,\mathrm{m^2\,s^{-2}}$	Velocity profile, $z_i = 500$ m and velocity variance $= 1.64\,\mathrm{m^2\,s^{-2}}$

In the left column, the names of the SCIPUFF configurations are given. "BL" stands for boundary layer in the naming convention. Surface heat flux is calculated by SCIPUFF for all configurations. Unless specified in the table, z_i (boundary layer depth) is also calculated by SCIPUFF. When z_i and/or surface heat flux are computed by SCIPUFF, the Bowen ratio and albedo were set for daytime (3 pm local time) urban winter conditions with no clouds overhead. Specifically, Bowen ratio = 1.5, albedo = 0.35 (Sykes et al., 1997) and cloud cover = 0. The variance supplied to the BLCFDv run had an imposed length scale of 12 m (twice the FAST3D-CT grid resolution).

height-averaged velocity variance was provided in addition to the specifications of "BLCFD".

The dosages (time-integrated concentrations) near the ground from the CFD model form complex distributions as a function of horizontal location (Figs. 4 and 5). On the CFD grid, at distances close to the source, contaminant fate is strongly influenced by the buildings and the patterns that evolve can be highly sensitive to the release site and the downwind building geometry. For instance, in Chicago, a release at r1 leads to a channeling of contaminant down the Chicago River. Pressure effects along the Chicago River are likely responsible for inhibiting the spread of the predicted contaminant to the north of the river. This stands in stark contrast to the outcome of a release at r4 where the contaminant becomes trapped in the interstitial regions between the tall, densely spaced buildings. Similarly, in Washington DC, a release at r1 culminated in the simulated agent being funneled down a major thoroughfare; whereas for a release at r4, the contaminant disperses amongst the wide spaces between buildings. In the simulations for both cities, the contaminant becomes trapped in vortices that form in the lee of buildings, the dynamics of which were first mapped out by Hosker (1984) using wind tunnel experiments. The variations in the simulated plume shapes correspond clearly to the variations in geometry. For an interior urban release such as r4, a rough characterization of plume spread angles suggests approximately 160° for Chicago and 45° for Washington DC.

The ensemble-average SCIPUFF version 1.3 simulations lead to dosage patterns generally in the shape of ovals that fan out at the downwind edge—here displayed superimposed over the urban grids for Washington DC and Chicago for reference (Fig. 6). The shape and extent of the plume is determined by the meteorology and the constant roughness factor for the surface. So local building geometry variations enter only through the average roughness coefficients. In subsequent sections we quantify the differences between the CFD and puff

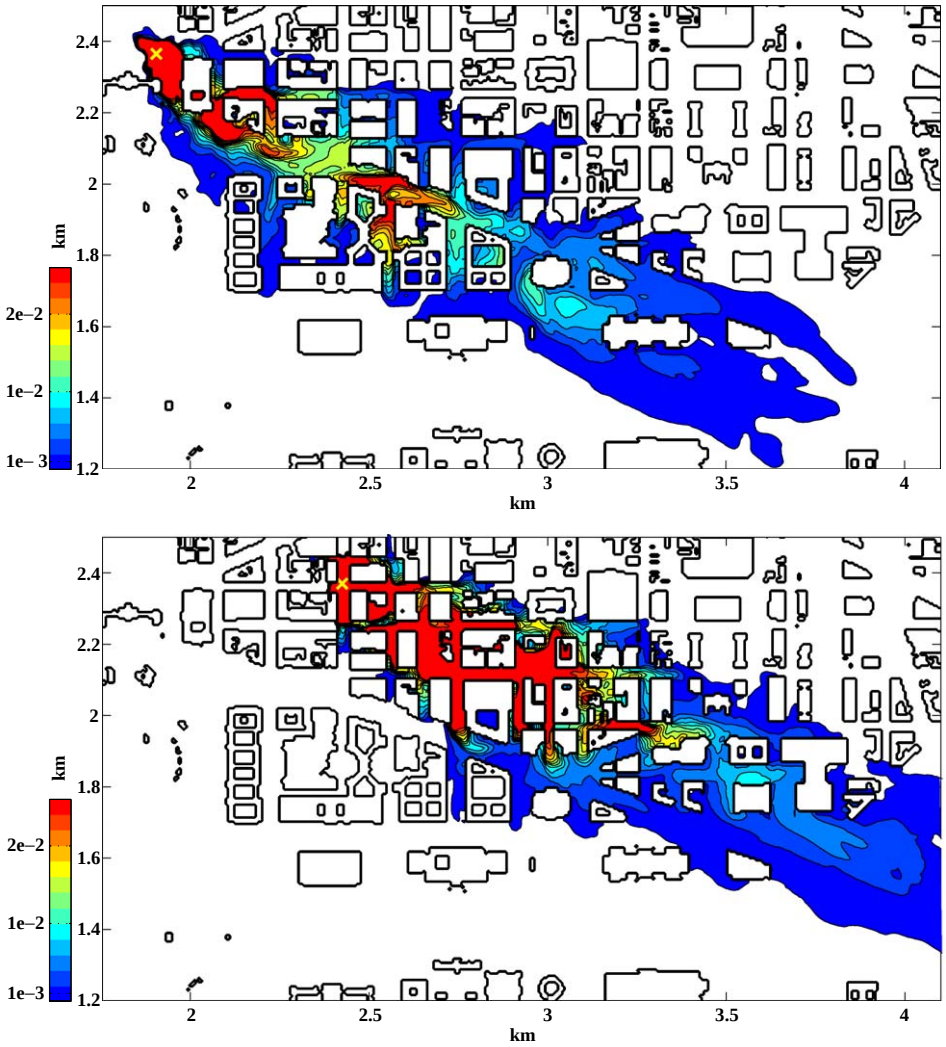

Fig. 4. FAST3D-CT Washington DC 1-m dosage (kg s m^{-3}) after 12 min, for two different release sites, r1 (above) and r4 (below), marked with yellow crosses. Only a 3 km^2 portion of the full grid is shown.

model dosage patterns that evolve near the ground within several kilometers of the source, integrated out to 12 and 18 minutes post-release.

3. Fine-grain statistics

Many studies have employed various metrics for evaluating model performance. There is a canonical set of performance measures that are finding increasing use in the air pollution literature (Hanna, 1994). Here, we assess the performance of the Gaussian puff model relative to the CFD model, in a model-to-model comparison, by using these standard statistical measures. The measures are applied to all dosage values that exceed a given background level. For illustrative purposes we examine the distribution pattern within the lowest dose contour shown in Figs. 4–6. That threshold is the contour level 0.001 kg s m^{-3}. In a real scenario, the contour of interest would depend on health or environmental effects. In order to assess dosage values on the same grid, SCIPUFF values were interpolated onto the CFD grid. Statistics were computed over the cell locations where there are no buildings. Basic statistics of mean, standard deviation and contaminated area (defined by the perimeter of the threshold dosage) that are generated by a given model (FAST3D-CT, noBL10m, noBL35m, BLCFD, and BLCFDv) are presented first (Fig. 7), followed by comparison statistics that relate FAST3D-CT dosages

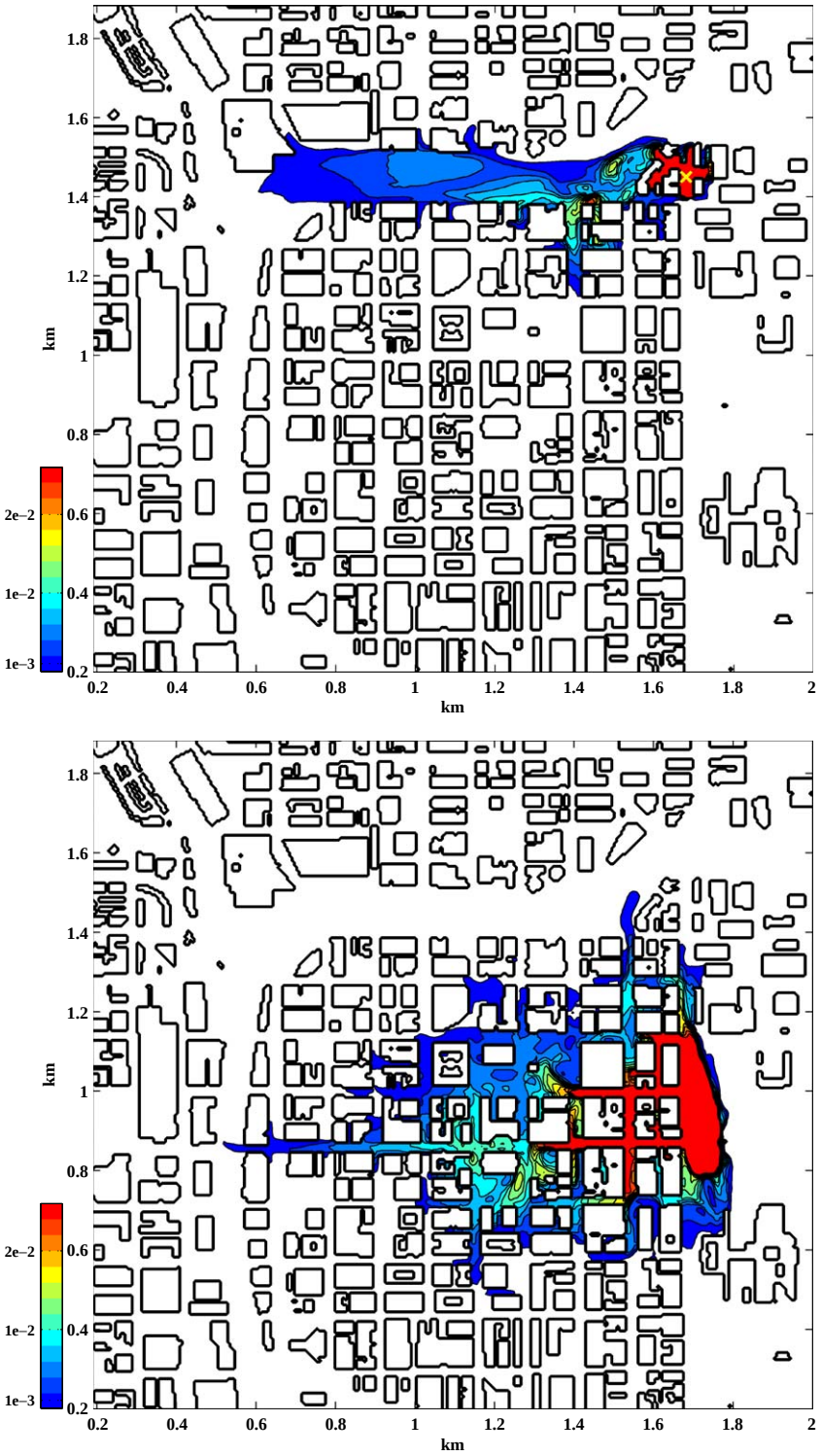

Fig. 5. FAST3D-CT Chicago 3-m dosage (kg s m^{-3}) after 12 min, for two different release sites, r1 (above) and r4 (below), marked with yellow crosses. Only a 3 km^2 portion of the full grid is shown.

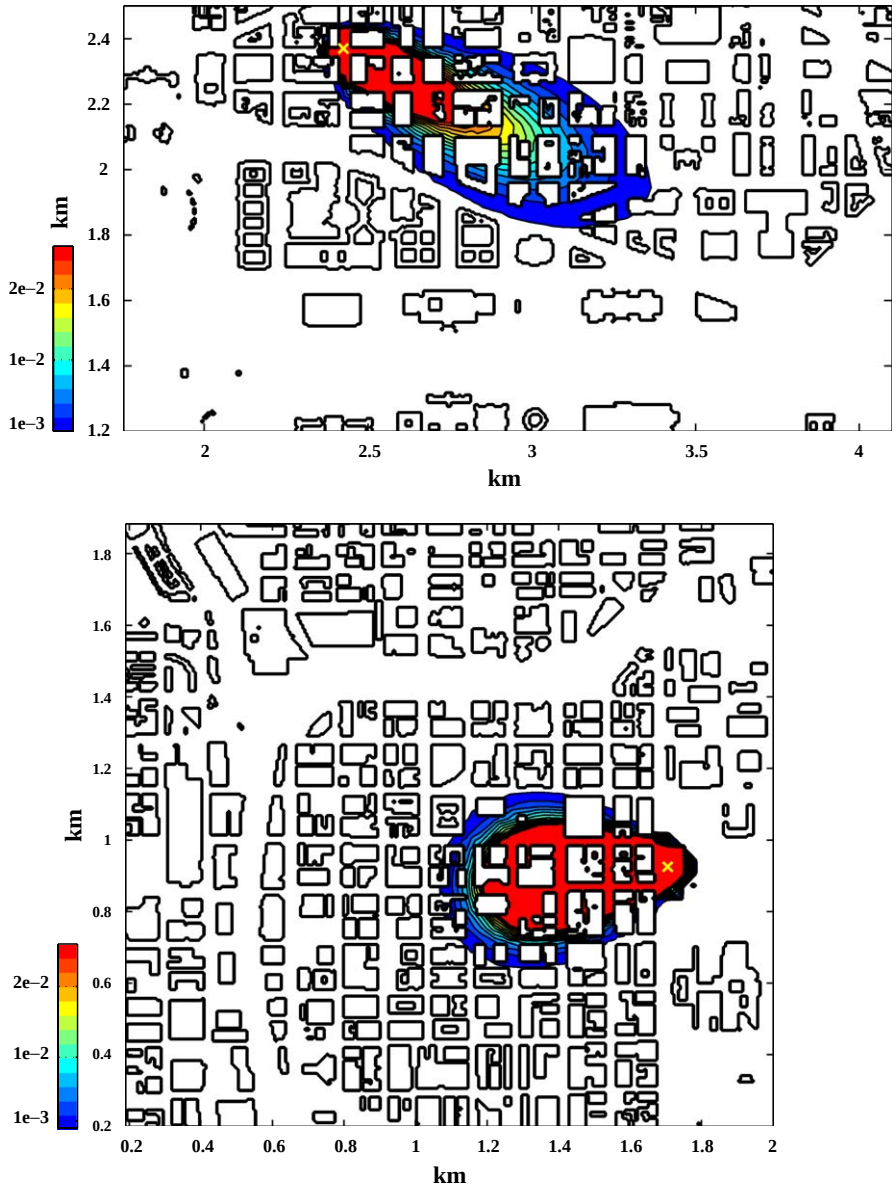

Fig. 6. Washington DC 1-m (top) and Chicago 3-m (bottom) dosage ($kg\,s\,m^{-3}$) after 12 min for SCIPUFF using BLCFD with a release at site r4 on each grid.

point-wise to corresponding values from the SCIPUFF simulations.

The statistics computed for each model reveal that the contaminated area is larger for the Washington DC FAST3D-CT simulation, relative to all SCIPUFF simulations, and these contaminated cells consistently have somewhat greater mean (except for r4) and substantially greater fluctuating values than are found in the Gaussian puff model. This conclusion holds for all permutations of weather information given to SCIPUFF from FAST3D-CT. Incidentally, the large standard deviation on the CFD grid is due to large dosage values in the immediate vicinity of the release at this low height above ground. This will be addressed below. As SCIPUFF receives more information about the simulated urban boundary layer flow, the contaminated region where dosage values exceed $0.001\,kg\,s\,m^{-3}$ expands.

By contrast, the FAST3D-CT Chicago simulation had among the lowest mean dosage values. It displayed greater fluctuations relative to all SCIPUFF configurations only for r1. Contaminated areas were generally

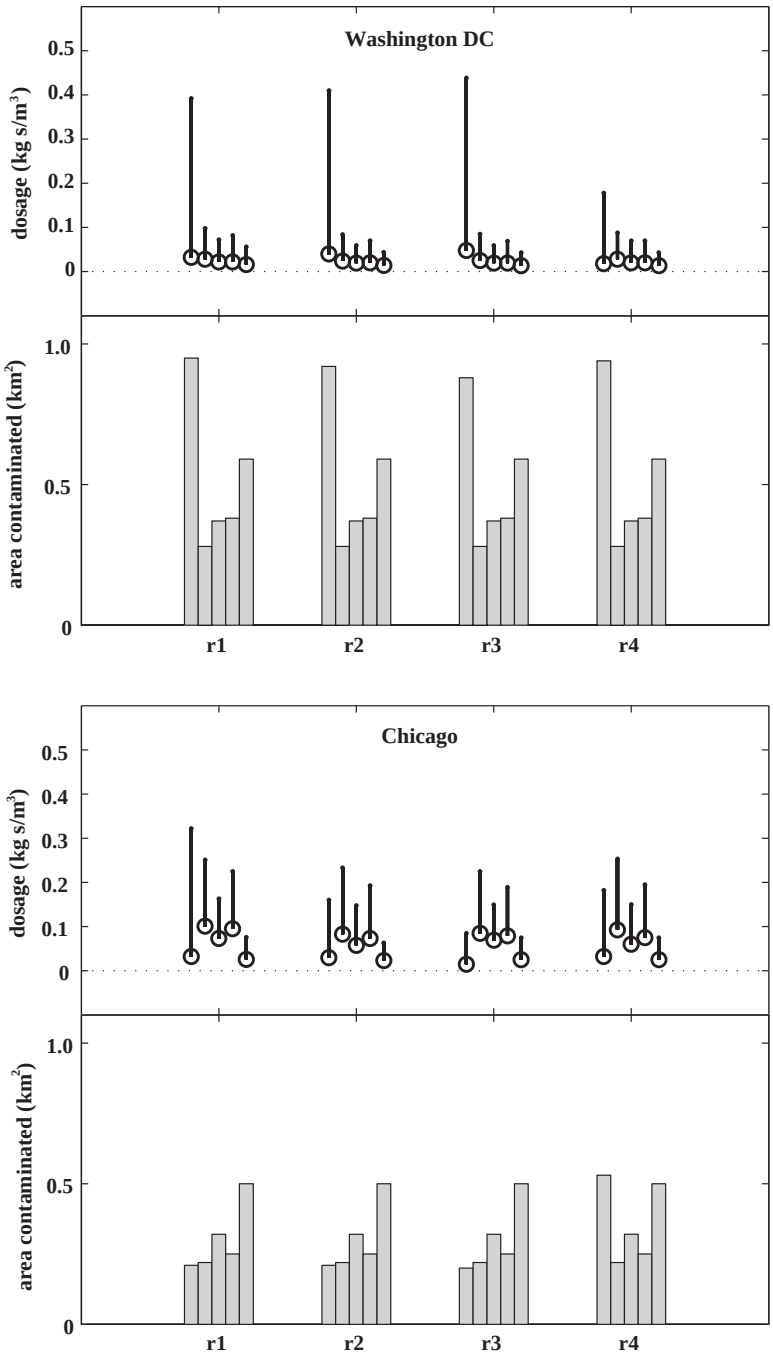

Fig. 7. Mean (open circles), one-sided standard deviation (lines), and area contaminated (bar graph). Each entry from left to right represents, respectively, FAST3D-CT, noBL10m, noBL35m, BLCFD, and BLCFDv simulations of Washington DC (top panels) and Chicago (bottom panels) after 12 min.

largest for BLCFDv, and FAST3D-CT values were only comparable to these areas for r4. FAST3D-CT dosage standard deviations and contaminated areas are more variable amongst the four release sites of Chicago as compared to Washington DC. FAST3D-CT and SCIPUFF discrepancies are generally associated with urban morphology and boundary layer effects. Dosage statistics at 18 min post-release for both cities follow the

trends outlined above, although the contaminated region is enlarged at 18 min relative to the earlier time.

Differences in near-surface FAST3D-CT contaminant distributions in Washington DC relative to Chicago may be attributed to the deeper boundary layer that develops in the Chicago simulation (with enhanced vertical mixing distributing the contaminant through the air column), coupled with more densely packed buildings in Chicago that limit the volume that the contaminant can occupy. This often leads to more lateral spreading of the contaminant and reduced mean dosage.

Differences in SCIPUFF near-surface contaminant distributions between Washington DC and Chicago are due to the urban meteorology. Lighter winds in the lower part of the boundary layer in the Chicago simulation presumably encourage contaminant accumulation near the surface for noBL10m, noBL35m and BLCFD. The greater variance in the wind field in BLCFDv serves to spread out the agent as seen by the lower mean and fluctuating dosage values and larger contaminated areas in Washington DC and Chicago relative to the other SCIPUFF configurations.

Comparison statistics of the SCIPUFF (all configurations) dosage values relative to FAST3D-CT are computed using a range of different metrics (Tables 2,3 and Appendix A). The assessment of individual cell values constitutes a "fine-grain" analysis, as it is focused on comparing local, point-to-point details of the dosage distributions. The number N represents the union of open (building free) cells that have dosage values exceeding the threshold, for FAST3D-CT or SCIPUFF—where dosage values below the threshold were set to zero. In addition, the few cells where FAST3D-CT values exceeded three standard deviations (where the standard deviation is shown in Fig. 7) were excluded from the comparison. This was done to address the stagnation of velocity near the ground that led to trapping of the contaminant in the immediate vicinity of the source site in the bottom grid cell of the CFD model.

Mean difference and fractional bias measure the model bias, while root mean square error and FAC2 quantitatively assess the model scatter. The correlation coefficient and index of agreement measure the overall agreement between the models. Results from these statistics are highly dependent on city, release site, and time post-release.

Over the region where either FAST3D-CT or SCIPUFF (or both) predicts contamination, SCIPUFF produces smaller mean values than FAST3D-CT for all meteorological input for Washington DC at both times. According to the MD and FB statistics, this deficit is most pronounced at both times for r3. Lowest magnitudes of MD and FB are found at r1 (both times). By contrast, the SCIPUFF Chicago releases have larger mean dosages at both times and all releases. For both times this excess dosage is largest (as measured by MD and FB) for r1 and r3 and smallest for r4. In terms of differences amongst the SCIPUFF configurations, BLCFDv has the smallest absolute value of MD and FB consistently for all release sites and times for Washington DC and Chicago. The differences between Washington DC and Chicago comparison statistics is consistent with the basic model statistics and interpretation presented earlier.

At both times, greatest SCIPUFF differences from the Washington DC FAST3D-CT dosage values (RMSE) are found for r2 and r3, while closest agreement is found for r1 and r4. The RMSE values for SCIPUFF configurations are generally comparable, with BLCFDv showing a slightly lower value at one release site (r2 at 12 min and r3 at 18 min). For Chicago at both times, largest RMSE are found for r1 and r3 with smallest values found for r4. Within SCIPUFF simulations, RMSE values are smallest using BLCFDv for all release sites and times for Chicago. FACT2 values are more variable and the trends are harder to discern. The most notable feature for Washington DC is that the largest percentage of SCIPUFF points lie within a factor of 2 of values from FAST3D-CT when using BLCFDv at both times. For Chicago, this holds true only after 18 min have elapsed (but not for r2).

For Washington DC, spatial correlation coefficients and index of agreement values are typically greatest for r1 at both times. In the Chicago simulations, largest correlation and index of agreement values occur for r4 at 12 min. At 18 min, the largest correlations are for r1 and the greatest IOAs occur for r4. Poorest correlations and lowest IOAs occur in Chicago for r3 (both times). Within SCIPUFF simulations, BLCFDv has the largest correlations for Chicago for all times and releases. For Washington DC, the same trend obtains save for r1 (both times).

For both cities, better statistical agreement was promoted by including more urban boundary layer information as input to SCIPUFF. The average correlation for BLCFDv for all release sites at 18 min post-release is 0.44 (0.68) for Chicago (Washington DC). The average FAC2 value for BLCFDv for all release sites at 18 min post-release is 17.08% (34.64%) for Chicago (Washington DC). Despite the improved agreement over the simpler specifications, the BLCFDv simulation for Chicago still has quite low FAC2 and correlation values. Circulations induced by local features such as the Chicago River that are represented by FAST3D-CT but not by SCIPUFF are likely responsible for the large discrepancies between the models, and certainly account for the large differences seen in FAST3D-CT plumes. Though BLCFDv correlations for Washington DC are moderately high, FAC2 values are all less than 40%—indicating a divergence in how

Table 2
Model dosage comparison statistics at 12 and 18 min post-release (Washington DC)

	N	MD	FB	RMSE	FAC2	CC	IOA
At 12 min[a]							
release 1							
noBL10m	19,276	−0.004	0.47	0.03	11.22	0.74	0.80
noBL35m	18,908	−0.003	0.43	0.03	16.26	0.73	0.78
BLCFD	19,077	−0.003	0.41	0.03	17.47	0.76	0.80
BLCFDv	21,107	−0.002	0.26	0.03	19.95	0.70	0.73
release 2							
noBL10m	16,920	−0.011	1.03	0.06	11.82	0.58	0.55
noBL35m	16,906	−0.011	0.98	0.06	12.90	0.50	0.48
BLCFD	16,902	−0.011	0.98	0.06	14.13	0.58	0.53
BLCFDv	17,893	−0.010	0.88	0.05	17.60	0.68	0.55
release 3							
noBL10m	16,512	−0.015	1.24	0.06	8.66	0.63	0.48
noBL35m	16,441	−0.014	1.16	0.06	12.98	0.60	0.46
BLCFD	16,473	−0.014	1.18	0.06	12.37	0.60	0.44
BLCFDv	17,453	−0.013	1.08	0.06	17.54	0.65	0.45
release 4							
noBL10m	18,483	−0.005	0.66	0.02	7.19	0.58	0.73
noBL35m	18,239	−0.005	0.58	0.02	8.51	0.56	0.72
BLCFD	18,348	−0.005	0.61	0.02	8.91	0.61	0.75
BLCFDv	20,289	−0.004	0.55	0.02	12.37	0.70	0.81
At 18 min[b]							
release 1							
noBL10m	21,248	−0.003	0.44	0.03	18.03	0.74	0.80
noBL35m	20,839	−0.003	0.39	0.03	25.19	0.73	0.78
BLCFD	21,140	−0.002	0.27	0.03	33.27	0.76	0.80
BLCFDv	24,844	−0.001	0.15	0.03	30.22	0.70	0.74
release 2							
noBL10m	18,910	−0.011	1.00	0.05	15.80	0.58	0.56
noBL35m	19,358	−0.011	0.94	0.05	28.25	0.50	0.48
BLCFD	19,223	−0.010	0.85	0.05	37.11	0.57	0.54
BLCFDv	21,650	−0.008	0.76	0.05	38.17	0.68	0.56
release 3							
noBL10m	17,422	−0.015	1.19	0.06	11.16	0.64	0.48
noBL35m	17,487	−0.015	1.11	0.06	27.01	0.62	0.47
BLCFD	17,867	−0.014	1.02	0.06	37.70	0.61	0.44
BLCFDv	21,311	−0.011	0.93	0.05	39.36	0.67	0.45
release 4							
noBL10m	20,038	−0.007	0.77	0.02	7.85	0.57	0.71
noBL35m	19,976	−0.007	0.68	0.02	18.18	0.55	0.71
BLCFD	20,054	−0.006	0.60	0.02	28.05	0.60	0.74
BLCFDv	24,182	−0.005	0.54	0.02	30.81	0.68	0.79

N = number of points where there are no buildings, and either SCIPUFF or FAST3D-CT dosage exceeds 0.001 kg s m^{-3}; MD = mean difference; FB = fractional bias; RMSE = root mean square error; FAC2 = percentage of points within a factor of 2 of the FAST3D-CT values; CC = correlation coefficient; IOA = index of agreement. Full definitions are given in Appendix A.

[a]For r1–r4, respectively, the number of excluded points (see text) is: 93, 105, 129, 71.

[b]For r1–r4, respectively, the number of excluded points (see text) is: 95, 108, 131, 75.

Table 3
Model dosage comparison statistics at 12 and 18 min post-release (Chicago)

	N	MD	FB	RMSE	FAC2	CC	IOA
At 12 min[a]							
release 1							
noBL10m	6164	0.056	−1.60	0.14	4.23	0.33	0.24
noBL35m	6983	0.056	−1.65	0.11	7.68	0.23	0.21
BLCFD	6419	0.063	−1.65	0.13	6.33	0.28	0.21
BLCFDv	10144	0.019	−1.37	0.04	5.98	0.51	0.58
release 2							
noBL10m	6011	0.034	−1.36	0.11	5.67	0.20	0.23
noBL35m	7068	0.034	−1.43	0.08	7.23	0.08	0.18
BLCFD	5939	0.038	−1.41	0.10	11.21	0.14	0.20
BLCFDv	8886	0.014	−1.12	0.04	8.29	0.36	0.51
release 3							
noBL10m	5669	0.047	−1.71	0.13	3.19	−0.06	0.02
noBL35m	6761	0.048	−1.76	0.09	3.77	−0.10	0.02
BLCFD	5799	0.051	−1.74	0.11	5.92	−0.08	0.02
BLCFDv	8735	0.020	−1.59	0.05	6.96	0.03	0.09
release 4							
noBL10m	8501	0.014	−0.55	0.09	13.02	0.48	0.52
noBL35m	9213	0.015	−0.62	0.07	12.27	0.33	0.48
BLCFD	8505	0.015	−0.59	0.08	14.15	0.43	0.52
BLCFDv	9810	0.002	−0.14	0.03	36.43	0.65	0.78
At 18 min[b]							
release 1							
NoBL10m	13,124	0.038	−1.50	0.10	4.89	0.54	0.27
NoBL35m	13,173	0.044	−1.56	0.08	8.81	0.43	0.26
BLCFD	13,185	0.042	−1.55	0.10	6.53	0.51	0.26
BLCFDv	17,997	0.013	−1.16	0.03	15.93	0.71	0.66
release 2							
NoBL10m	10,332	0.035	−1.55	0.10	11.05	0.15	0.13
NoBL35m	13,009	0.031	−1.59	0.07	8.62	0.09	0.11
BLCFD	10,475	0.036	−1.57	0.09	11.58	0.14	0.13
BLCFDv	15,672	0.012	−1.28	0.03	9.94	0.36	0.44
release 3							
NoBL10m	8952	0.048	−1.79	0.12	6.52	−0.09	0.01
NoBL35m	12,274	0.040	−1.81	0.08	5.06	−0.10	0.01
BLCFD	9511	0.049	−1.80	0.10	6.10	−0.09	0.01
BLCFDv	14,805	0.016	−1.64	0.04	9.91	0.02	0.07
release 4							
noBL10m	12,215	0.020	−0.84	0.08	13.94	0.47	0.44
noBL35m	15,390	0.018	−0.91	0.06	8.59	0.33	0.42
BLCFD	12,529	0.021	−0.87	0.07	15.28	0.43	0.45
BLCFDv	15,892	0.004	−0.33	0.02	32.53	0.65	0.78

N = number of points where there are no buildings, and either SCIPUFF or FAST3D-CT dosage exceeds 0.001 kg s m^{-3}; MD = mean difference; FB = fractional bias; RMSE = root mean square error; FAC2 = percentage of points within a factor of 2 of the FAST3D-CT values; CC = correlation coefficient; IOA = index of agreement. Full definitions are given in Appendix A.

[a]For r1–r4, respectively, the number of excluded points (see text) is 35, 95, 52, 121.

[b]For r1–r4, respectively, the number of excluded points (see text) is 43, 122, 64, 147.

FACT3D-CT and SCIPUFF distribute the contaminant within the threshold dosage contour.

4. Coarse-grain statistics

Warner et al. (2004a) have developed an area-based measure of effectiveness (MOE) to characterize the overlap and size of predicted hazard regions. We adopt this measure here to quantify the degree to which the puff and CFD model cover comparable areas (in size) and extend over the same region (in space). At two times for all models and all release sites, the total area contained within the $0.001\,\mathrm{kg\,s\,m^{-3}}$ contour (the same threshold used in Section 3) is computed. (The choice of this dosage threshold is somewhat arbitrary. Note that some of the areas used in this computation were presented graphically in Fig. 7.) The region of overlap of the area contained within the threshold contour of the FAST3D-CT and SCIPUFF permutations is calculated. The two-dimensional MOE plots of $\mathrm{Area_{overlap}}/\mathrm{Area_{SCIPUFF}}$ (abscissa) vs. $\mathrm{Area_{overlap}}/\mathrm{Area_{FAST3D\text{-}CT}}$ (ordinate) are formed (Figs. 8 and 9). Along the diagonal (dashed line) hazard areas for the two models are the same size but overlap only partially—e.g., the location ($x = 0.5$, $y = 0.5$) would represent a 50% overlap. At the upper right corner ($x = 1.0$, $y = 1.0$) the areas are the same size and they overlap

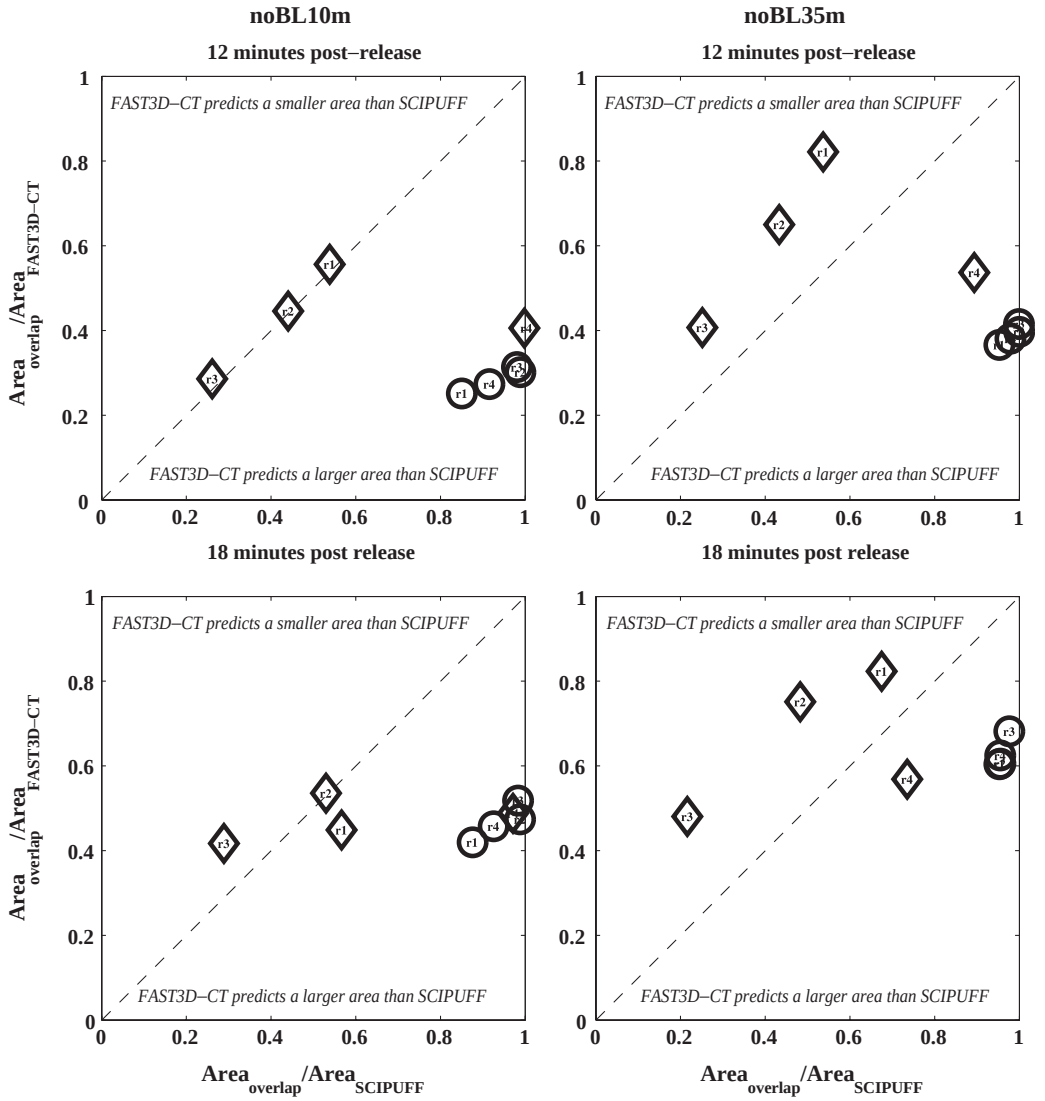

Fig. 8. Area-based measure of effectiveness plots for the Washington DC (circles) and Chicago (diamonds) simulations. There is a data point for each release site (r1–r4). Here the two simplest SCIPUFF configurations are shown.

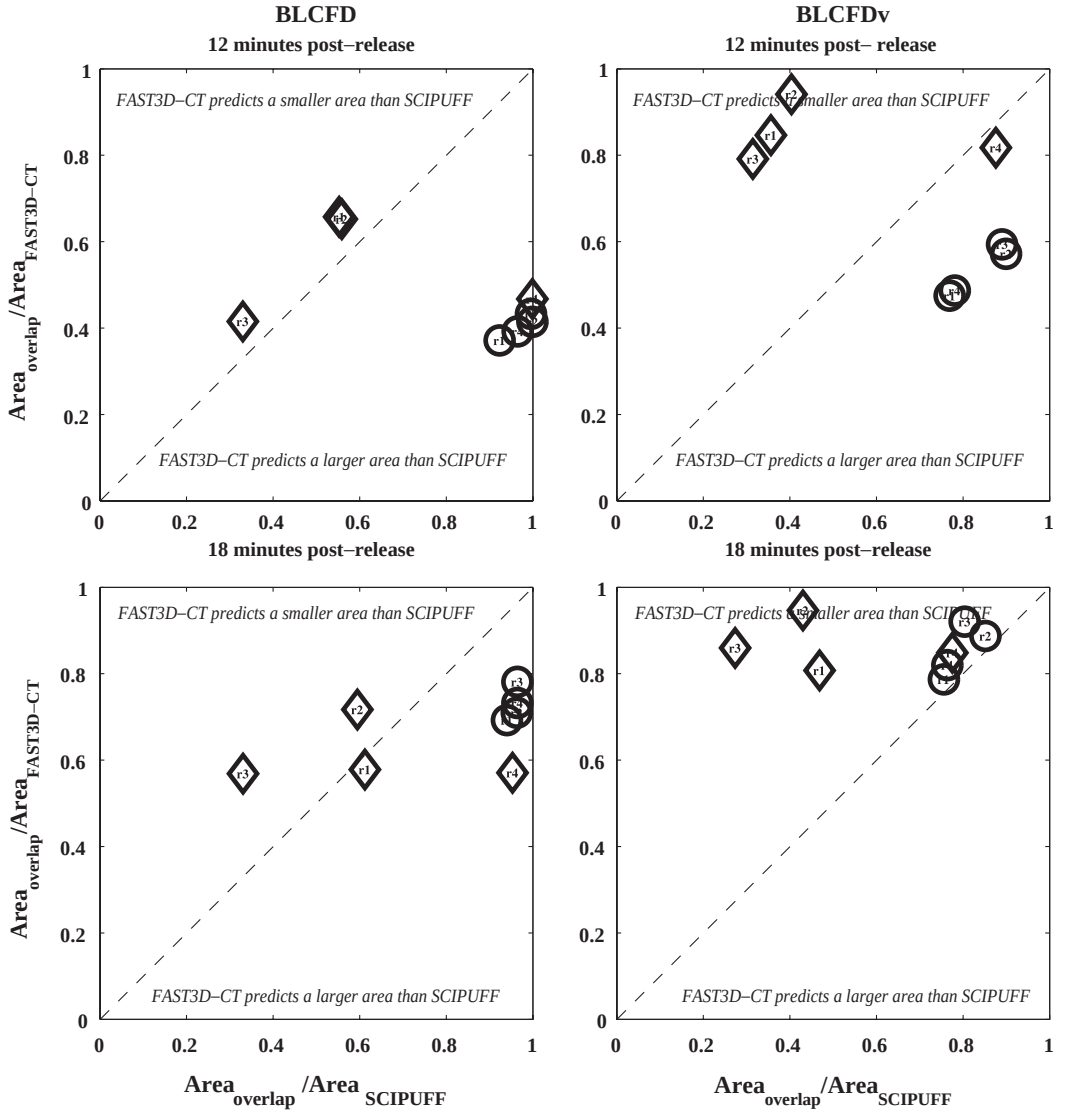

Fig. 9. As in Fig. 8, but for the two advanced SCIPUFF configurations.

entirely—i.e., they are identical plumes. Below the diagonal, FAST3D-CT predicts a larger area, while above the diagonal, SCIPUFF forecasts a larger area.

The MOE statistic, defined above, for the Washington DC simulation (circles) reveals that the noBL10m and noBL35m SCIPUFF results cover a smaller area than FAST3D-CT, but over time the overlap region expands to cover an increasing fraction of the FAST3D-CT area (Fig. 8). Note that an abscissa value ($Area_{overlap}/Area_{SCIPUFF}$) of 1.0 means that the SCIPUFF area is entirely contained within the overlap region. This occurs for several release sites. BLCFD MOE values are located even closer to the diagonal line, and for BLCFDv, SCIPUFF just barely covers more area than FAST3D-CT for all release sites at 18 min post-release (Fig. 9). An important feature of these graphs is that the hazard area statistics produced by all four Washington DC release sites tend to cluster close to each other.

The hazard areas for the Chicago simulation (diamonds) have markedly different characteristics. In particular, for noBL10m, three of the four release sites (r1–r3) lead to approximately the same size release as FAST3D-CT, although the degree of overlap with FAST3D-CT varies (Fig. 8). The anomalous SCIPUFF hazard region (corresponding to release site r4) is entirely contained within the FAST3D-CT contaminated region. For noBL35m, SCIPUFF areas are larger than FAST3D-CT areas for r1–r3. However, it requires

the full suite of urban meteorological information, BLCFDv, for SCIPUFF plumes from all release sites to come closest to containing the FAST3D-CT-generated contaminated areas (Fig. 9). This occurs at 18 min post-release. A salient feature of the Chicago simulations is the large variations in the hazard size and degree of overlap as a function of specific release location in FAST3D-CT results.

Chicago has taller, more variable, and denser buildings than Washington DC. In fact, the mean Chicago building height is almost three times that of Washington DC, while the standard deviation of Chicago building height is close to five times that of Washington DC. Buildings cover ten percent more of the area on the Chicago grid compared to an equivalent area on the Washington DC grid.

The meteorological inputs to SCIPUFF were different for the two cities. The Chicago simulation, possessing a greater average building height, developed a deeper boundary layer than the Washington DC simulation. And the winds attained a greater magnitude in the bottom part of the boundary layer on the Washington DC grid compared to the Chicago grid.

In Section 3, the fine-grain statistics revealed better model agreement for Washington DC compared to Chicago. Indeed, the average BLCFDv 18 min post-release FAC2 value of all four hypothetical release sites increased by 103% in Washington DC relative to Chicago. Likewise, the correlation coefficient increased by 55%. The fine-grained and coarse-grain statistics both suggest that the tall and highly corrugated urban landscape of Chicago reduces predictability and

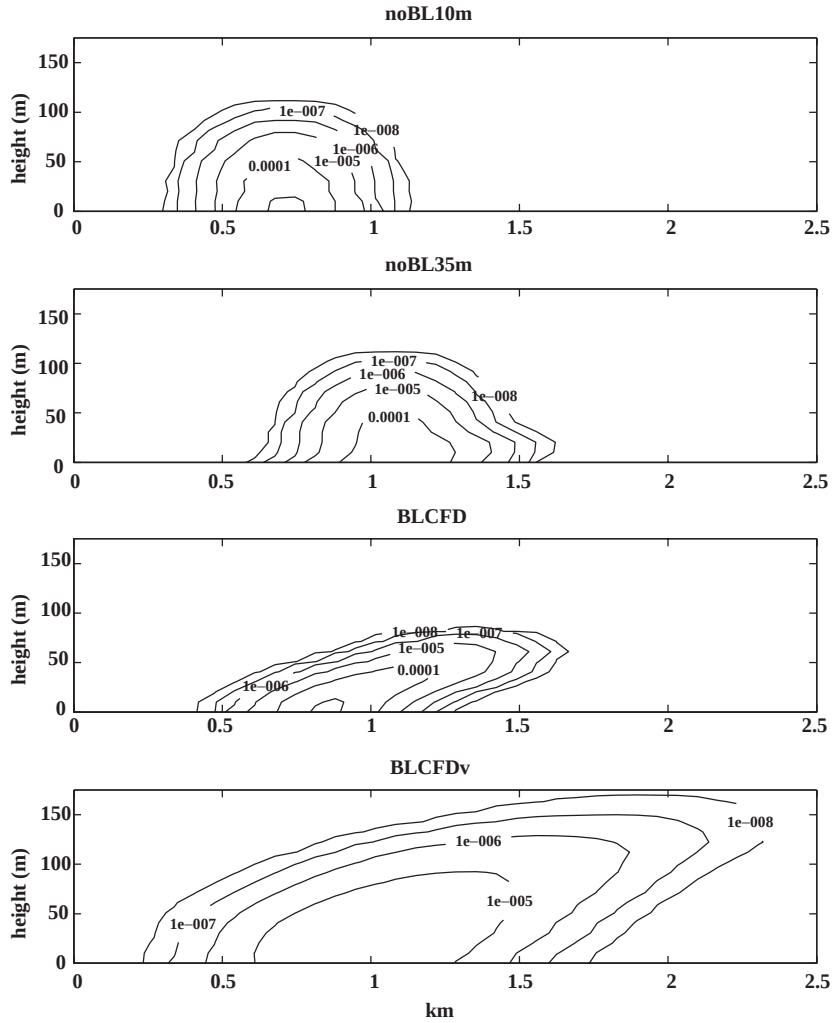

Fig. 10. Chicago SCIPUFF agent concentration (kg m^{-3}) on a vertical section along the middle of the downwind axis at 12 min post-release.

increases sensitivity to release site relative to the lower and more uniform urban profile presented by Washington DC.

For both cities, for all release sites and all SCIPUFF variations, there is a marked general model-to-model agreement of coarse-grain statistics as time progresses, and as more meteorological information is supplied to SCIPUFF. This topic will be explored in the next section.

5. Boundary layer considerations

Animations of a number of FAST3D-CT simulations show the contaminant lofting aerodynamically as it encounters buildings. The elevated mixing generated by flows in urban areas was recognized by Hosker (1984). And the "fountain" effect was explained by Boris (2002). These effects are illustrated in Fig. 4. The lofting injects the contaminant into a faster part of the boundary layer and permits transport to greater distances downwind immediately following release.

There is enhanced agreement with the CFD model, using both fine and coarse grained statistics, in the Chicago and Washington DC simulations of the SCIPUFF configuration that received full information about the urban meteorology (BLCFDv). Vertical sections of agent concentration along the axis of the plume for the SCIPUFF variations at 12 min post-release reveal the height-dependent transport in the boundary layer (Fig. 10). Specifically, for the Washington DC (not shown) and Chicago simulations, the noBL10m and noBL35m runs of SCIPUFF receive a velocity from the lower part of the boundary layer that tends to confine the agent to a lump that translates laterally. This distribution travels faster in the noBL35m simulation because the CFD-derived velocity is swifter higher in the boundary layer, at 35 m compared to 10 m.

By contrast the BLCFD and BLCFDv simulations have contaminant concentrations that reflect the sheared flow in the boundary layer that evolves on the CFD grid due to the presence of the buildings (Figs. 2 and 3). The lofting "fountain" effect that is generated on the CFD grid by the interaction of the finely resolved fluid dynamics with the building morphology leaves an imprint on the area-averaged CFD velocity profile, which the BLCFD and BLCFDv configurations of SCIPUFF inherit. Similar results were obtained at 18 min post-release. It was only at this later analysis time that all of the SCIPUFF BLCFDv plumes were at least as large as the FAST3D-CT-predicted hazard areas. This suggests that the FAST3D-CT downwind agent transport was still quicker than that represented by SCIPUFF with the most urban boundary layer information. And therefore this rapid vertical and downwind contaminant projection could put urban populations at large distances at risk more quickly than anticipated by operational plume models. However, once a plume has had sufficient time to spread out, the effect of the individual buildings on the contaminant fate is less pronounced, and an appropriate area-averaged representation of the velocity profile (and velocity fluctuations) is capable of generating realistic plume dimensions in a simple puff model. This assessment will be extended in Section 6.

6. Discussion and conclusions

A major goal of this work was to quantify the impact of urban effects on plume shape and size. In this study we have used a building-resolving CFD model (FAST3D-CT) that simulates realistic features of urban flow. These include urban canyon effects, building-specific lofting, and eddies in the wakes of buildings. We assessed the performance of a Gaussian puff model (SCIPUFF) relative to the performance of the high-resolution urban CFD model.

Strictly speaking, puff model results are considered valid in the far field, beyond several building heights. The results of our work suggest a guideline for deciding when Lagrangian methods, based on approximations that ignore vortex shedding at altitude (i.e. from the tops of buildings) or do not treat the full time dependence of the turbulence, can be used. The effect of individual buildings on the CFD solution becomes smoothed out at a distance where the lateral extent of the plume is at least eight to ten times its height at least three quarters of the way downwind from the source. In typical FAST3D-CT simulations this occurs when the plume is 4–5 km long and 30 min or more have passed. In the far-field of plumes displaying this ratio, the "random" walks of the contaminated air parcels in turbulent eddies start to take on the character of a diffusive process. At this scale, the physics encapsulated in simple plume models should approximate the coarse-grain statistical properties that can be rendered by a more detailed CFD model.

For evacuation planning purposes, a puff model may be capable of approximating the contaminated regions—provided it is supplied with accurate and specific information about the building-dominated urban boundary layer and sufficient time has elapsed post-release. However, in a simulation designed to mimic current widely used operational implementations (meteorology consisting of velocity at one height as represented here by configuration noBL10m, and evocative of a scenario where only airport meteorological station data is available), SCIPUFF predicted smaller contaminated regions in Washington DC for all release sites, and in Chicago for one to two release sites, out to at least ~20 min post-release. This result held even for the progressively more sophisticated

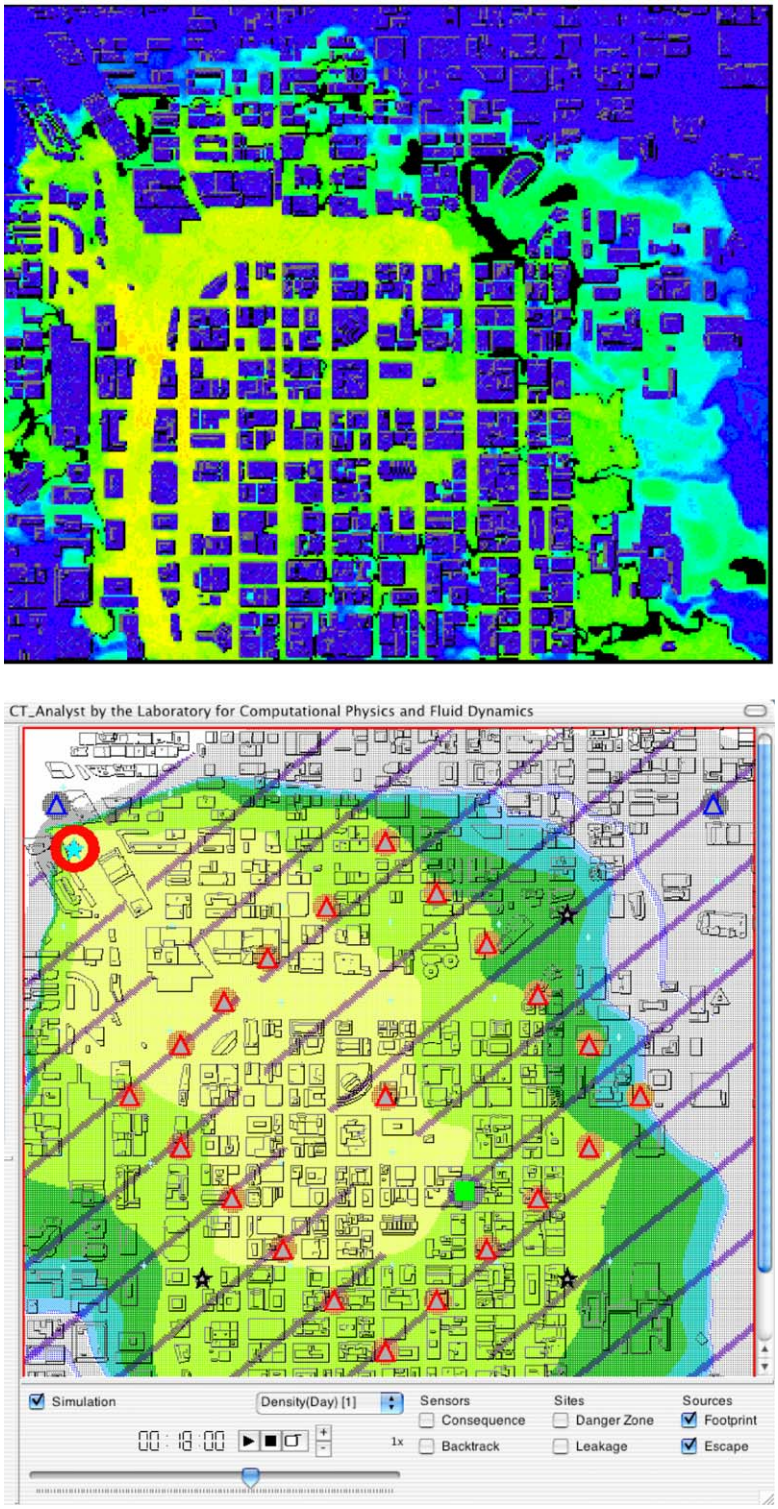

Fig. 11. A Chicago release in FAST3D-CT (top panel) and representation in CT-ANALYST (bottom panel). CT-ANALYST incorporates displays of plume envelopes (color contours), escape routes (diagonal lines), and sensor location/state (triangles).

meteorological specifications to SCIPUFF represented by noBL35m and BLCFD.

The SCIPUFF simulation that received the most knowledge of the simulated boundary layer structure (BLCFDv) produced fine-grain comparison statistics that were more consistent with the CFD model compared with noBL10m, noBL35m and BLCFD. That is SCIPUFF BLCFDv simulations came within a factor of 2 of the FAST3D-CT dosage values (or vice versa) for on average 17% (35%) of the contaminated Chicago (Washington DC) cells after 18 min. The Washington DC setting led to better correspondence between the CFD and Gaussian puff model compared with the Chicago locale. However, the overall agreement of the fine-grained statistics is not good for either city. In terms of the coarse-grain statistics, by incorporating successively more detailed information about the urban boundary layer that developed on the CFD grid, we found that SCIPUFF generated contaminant plumes that notably became larger than FAST3D-CT contaminated areas at later times, although they did not ever fully contain the FAST3D-CT contaminated regions.

We further deduce from the coarse-grain statistics that cities with high profile morphology and a great deal of variation (such as Chicago) produce hazard areas whose characteristics are quite sensitive to release location and meteorological conditions. By contrast, cities like Washington DC that have relatively low-building profiles spawn contaminated regions whose shape and size after a corresponding time, become relatively less dependent on the specific release location. These conclusions, based on this two-city comparison and reinforced by the fine-grain statistics, carry implications regarding relative predictability of contaminant plumes in urban landscapes.

In recognition of the importance of urban areas, SCIPUFF/HPAC is being extended phenomenologically through the Urban Wind Field Module (UWM) and the Urban Dispersion Model (UDM) to include approximations to some urban effects. These enhancements are not in general operational use, although they have been undergoing comparison testing. For instance Warner et al. (2004b) compared four urban HPAC configurations: urban HPAC (with urban SCIPUFF settings similar to those used here), UWM, UDM, and UWM with UDM. Surprisingly, the best overall correspondence with Urban 2000 Salt Lake City agent concentration data was obtained using urban HPAC—a configuration that in contrast to the others, did not contain any cognizance of building geometry. Further evaluation of the strengths and weaknesses of UWM and UDM appears warranted.

Alternately, there is a systematic way to capture much of the 3D nature of detailed CFD simulations in a form that is fast and easy to use. Because a FAST3D-CT simulation of 10 km^2 at 6 m resolution typically takes 8 h on a 16 processor computer, it is not yet possible to run FAST3D-CT in an operational framework. In a practical realization of a simplified approach, FAST3D-CT forms the foundation of a real-time system called CT-ANALYST (Boris et al., 2002) (Fig. 11). CT-ANALYST predicts hazard areas for a range of wind directions and magnitudes using pre-computed data from FAST3D-CT simulations. In addition, hazard areas can be further circumscribed by the incorporation of fused multisensor information when a release is detected. CT-ANALYST produces conservative estimates of plume areas that encompass all realizations of FAST3D-CT and agree well with the timing and location of contaminated regions from field-trial data (Boris et al., 2004).

Generating an ensemble of multiple realizations of FAST3D-CT leads to a robust characterization of hazard areas, as encapsulated in CT-ANALYST (Boris et al., 2004); whereas the simulations presented here contained one realization of a meteorological state for each city. In reality, urban meteorological conditions can be even more complex and variable due to processes such as frontal passages, sea breezes, and local air–sea interaction. A mesoscale model is required to resolve these effects (Cai and Steyn, 2000). Current work is underway to connect the Navy's Coupled Ocean/Atmosphere Mesoscale Prediction System (COAMPS™) (Hodur et al., 2001) with the urban CFD model utilized in this study (Boris, 2002).

The upcoming New York City Urban Dispersion Program (NYC UDP) is an opportunity to exercise modeling capabilities in a complex coastal regime. Simpler models have been run for NYC, including FLUENT (a steady-state CFD model) (Huber et al., 2004). As well, FAST3D-CT has been used to simulate several releases in NYC. The additional evaluation data from the field component of the program is eagerly awaited.

Detailed meteorological information allowed the puff model to approximately mimic the lofting effect of the flow that developed in the CFD model as the winds encountered buildings. This led to greater correspondence between the CFD model and the puff model in both fine and coarse grain statistics for the BLCFDv meteorological specification to SCIPUFF. It is essential for dispersion models to receive accurate, high-resolution spatial and temporal information about the winds in order to improve forecasts of contaminant fate—whether they are CFD or Gaussian puff models. In addition, this work points to the supplemental gains accrued by specifying higher-order information like boundary layer height, wind variability, and even spatially variable turbulence quantities to better constrain the forecast evolution of contaminant plumes.

Acknowledgements

J. Pullen was the recipient of a science fellowship at the Center for International Security and Cooperation (CISAC), Stanford University, during which time this work was completed. Thanks to Lynn Eden, Chris Chyba and Dean Wilkening of CISAC for their interest, support and enthusiasm regarding this work. Thanks to Bill Burnett for introducing the authors and for encouraging this work. We are appreciative of the careful reading and recommendations of an anonymous reviewer and Richard P. Signell, both of which improved this paper.

Appendix A

Following the equations presented by Hanna (1994) and applied by Svensson (1998) for urban air quality modeling, mean difference is defined as

$$MD = \overline{D_{\mathrm{SCIPUFF}} - D_{\mathrm{FAST3D}}}, \tag{A.1}$$

where D is dosage and an overbar denotes a spatial average over all N data points at one moment in time. Fractional bias is

$$\mathrm{FB} = \frac{1}{2}\frac{(\overline{D_{\mathrm{FAST3D}}} - \overline{D_{\mathrm{SCIPUFF}}})}{(\overline{D_{\mathrm{FAST3D}}} + \overline{D_{\mathrm{SCIPUFF}}})}. \tag{A.2}$$

While root mean square error is

$$\mathrm{RMSE} = \sqrt{\frac{1}{N}\sum_{i=1}^{N}(D_{\mathrm{SCIPUFF}} - D_{\mathrm{FAST3D}})^2} \tag{A.3}$$

and FAC2 is the percentage of SCIPUFF cells within a factor of 2 of the corresponding values on the FAST3D-CT grid

$$0.5 < D_{\mathrm{FAST3D}}/D_{\mathrm{SCIPUFF}} < 2. \tag{A.4}$$

The spatial correlation coefficient is calculated according to

$$\mathrm{CC} = \frac{\overline{(D_{\mathrm{FAST3D}} - \overline{D_{\mathrm{FAST3D}}})(D_{\mathrm{SCIPUFF}} - \overline{D_{\mathrm{SCIPUFF}}})}}{\sigma_{\mathrm{FAST3D}}\sigma_{\mathrm{SCIPUFF}}}, \tag{A.5}$$

where σ is the standard deviation. Finally, the index of agreement is defined as

$$\mathrm{IOA} = 1 - \frac{\sum_{i=1}^{N}(D_{\mathrm{SCIPUFF}} - D_{\mathrm{FAST3D}})^2}{\sum_{i=1}^{N}(|D_{\mathrm{SCIPUFF}} - \overline{D_{\mathrm{FAST3D}}}| + |D_{\mathrm{FAST3D}} - \overline{D_{\mathrm{FAST3D}}}|)^2}. \tag{A.6}$$

References

Allwine, K.J., Shinn, J.H., Streit, G.E., Lawson, K.L., Brown, M., 2002. A multiscale field study of dispersion through an urban environment. Bulletin of the American Meteorological Society 83, 521–536.

Boris, J.P., 2002. The threat of chemical and biological terrorism: preparing a response. Computing in Science and Engineering 4 (2), 22–32.

Boris, J.P., Grinstein, F.F., Oran, E.S., Kolbe, R.L., 1992. New insights into large eddy simulation. Journal of Fluid Dynamics Research 10 (4–6), 199–228.

Boris, J.P., Obenschain, K., Patnaik, G., Young, T.R., 2002. CT_Analyst: fast and accurate CBR emergency assessment. Proceedings of the First Joint Conference on Battle Management for Nuclear, Chemical, Biological and Radiological Defense, Williamsburg, VA.

Boris, J.P., Cheatham, S., Patnaik, G., Young, T., 2004. Variability, validation, and CFD: there is no truth. 8th Annual George Mason University Conference on Transport and Dispersion Modeling, Fairfax, VA, July 13–15, 2004.

Cai, X.-M., Steyn, D.G., 2000. Modelling study of sea breezes in a complex coastal environment. Atmospheric Environment 34, 2873–2885.

Emery, M., Chtchelkanova, A., Cybyk, B., Boris, J., Shinn, J., Gouveia, F., 2000. Detailed modeling of air flow around a complex building. Proceedings of the 3rd Symposium on the Urban Environment. American Meteorological Society, Davis, CA, pp. 58–59.

Fureby, C., Grinstein, F.F., 2002. Large eddy simulation of high-Reynolds-number free and wall-bounded flows. Journal of Computational Physics 181 (1), 68–97.

Grinstein, F.F., Fureby, C., 2002. Recent progress on MILES for high Reynolds number flows. Journal of Fluids Engineering 124 (4), 848–861.

Hanna, S.R., 1994. Mesoscale meteorological evaluation techniques with emphasis on needs of air quality models. In: Pielke, R.A., Pearce, R.P. (Eds.), Mesoscale Modeling of the Atmosphere. American Meterological Society, Boston MA, pp. 47–62.

Hodur, R.M., Pullen, J., Cummings, J., Hong, X., Doyle, J.D., Martin, P., Rennick, M.A., 2001. The coupled ocean/atmosphere mesoscale prediction system (COAMPS). Oceanography 15, 88–98.

Hosker, Jr., R.P., 1984. Flow and dispersion near obstacles. In: Randerson, D. (Ed.), Atmospheric Science and Power Production, US Department of Energy, Technical Information Center, DOE/TIC–2760 (DE 84005177), Oak Ridge, TN (Chapter 7).

Hosker, Jr., R.P., 1987. The effects of buildings on local dispersion. In: Modeling the Urban Boundary Layer. American Meteorological Society pp. 95–159.

Huber, A., Georgopoulos, P., Gilliam, R., Stenchikov, G., Wang, S.W., Kelly, B., Feingersh, H., 2004. Modeling air pollution from the collapse of the World Trade Center and assessing the potential impacts on human exposures. Environmental Manager 35–40.

Kim, J.-J., Baik., J.-J., 1999. A numerical study of thermal effects on flow and pollutant dispersion in urban street canyons. Journal of Applied Meteorology 38, 1249–1261.

Nappo, C.J., Eckman, R.M., Rao, K.S., Herwehe, J.A., Gunter, R.L., 1998. Second order closure integrated puff (SCIPUFF) model verification and evaluation study. NOAA Air Resources Laboratory, Silver Spring, MD 63pp.

National Research Council (NRC), 2003. Tracking and Predicting the Atmospheric Dispersion of Hazardous Material Releases: Implications For Homeland Security. National Academies Press, Washington DC, 114pp.

Office of the Federal Coordinator for Meteorology, 1999. Directory of Atmospheric Transport and Diffusion Consequence Assessment Models, FCM-I3-1999, Washington, DC, 272pp.

Oke, T.R., 1984. The energetic basis of the urban heat island. Quarterly Journal of the Royal Meteorological Society 108, 1–24.

Oke, T.R., Johnson, G.T., Steyn, D.G., Watson, I.D., 1991. Simulation of surface urban heat islands under 'ideal' conditions at night. Part 2: diagnosis of causation. Boundary-Layer Meteorology 56, 339–358.

Oran, E.S., Boris, J.P., 2001. Numerical Simulations of Reactive Flow. Cambridge University Press, New York 529pp.

Patnaik, G., Boris, J.P., Grinstein,F.F., Iselin, J.P., 2003. Large scale urban simulation with the MILES approach. Annual AIAA CFD Conference, AIAA Paper 2003-4104, Orlando FL.

Svensson, G., 1998. Model simulations of the air quality in Athens, Greece, during the MEDCAPHOT-TRACE campaign. Atmospheric Environment 32 (12), 2239–2268.

Sykes, R.I., et al., 1997. PC-SCIPUFF version 1.0 technical documentation. Titan Corporation, Princeton, NJ 125pp.

Warner, S., Heagy, J.F., Platt, N., Larson, D., Sugiyama, G., Nasstrom, J.S., Foster, K.T., Bradley, S., Bieberbach, G., 2001. Evaluation of transport and dispersion models: a controlled comparison of HPAC and NARAC predictions. IDA Paper P-3555.

Warner, S., Platt, N., Heagy, J.F., 2004a. User-oriented two-dimensional measure of effectiveness for the evaluation of transport and dispersion models. Journal of Applied Meteorology 43, 53–73.

Warner, S., Platt, N., Heagy, J.F., 2004b. Comparisons of transport and dispersion model predictions of the Urban 2000 Field Experiment. Journal of Applied Meteorology 43, 829–846.